BNL 9443

Conf-650806-13

Seventh International Conference
on Phenomena in Ionized Gases, 1965

ELECTRON DRIFT VELOCITY VARIATIONS IN NEON + 10% HELIUM + ALCOHOL, USING SPARK CHAMBER EFFICIENCY AS A SENSITIVE INDICATOR[1]

Joachim Fischer
Brookhaven National Laboratory
Upton, N. Y.

A B S T R A C T

The disappearance probability of an electron in a gas is very sensitive to variations in transport coefficients. The efficiency of a pulsed nuclear spark chamber is a non-ideal indicator of this probability. Efficiency measurements were used to obtain spark chamber resolving times and measure drift velocity variations in (Ne+10% He)+C_2H_5OH in a 6.4 mm gap at NTP at E/P of .1 to 2 V/cm/mmHg and vapor pressures of 6 to 48 mmHg. The drift velocities are higher than without alcohol, and show a peak which shifts to higher E/P and velocity with increasing alcohol. The observations are related qualitatively to the reduction of electron energy by alcohol and to changes in collision cross-sections of the gas components.

1 This work was done under the auspices of the U. S. Atomic Energy Commission.

DISCLAIMER

INTRODUCTION

The electron drift velocity is an important parameter in pulsed nuclear spark chambers /1/ because it determines the chamber memory or resolving time for successive particles. A spark chamber can be made sensitive to a single electron.

By measuring the sparking efficiency of the chamber at various delays and clearing fields one not only establishes the resolving time of the spark chamber but also obtains a more sensitive measure of the variation in drift velocity and other electron disappearance factors than is normally obtained by direct drift time observations of electron swarms.

Minima and maxima were found in sparking efficiency curves of neon + 10% helium + ethyl alcohol /2/ as a function of the field, drift time and alcohol concentration. The shape of the resultant drift velocity curves is discussed in relation to electron collision cross-sections in the components of the gas mixture.

APPARATUS

The system is shown by the upper diagram in Fig. 1. The spark chamber consisted of 2 aluminum /3/ foils, 0.18 mm thick, spaced by a glass cylinder about 5 cm diameter and 6.4 mm high. A flow of gas of one cm^3 or more per second was purified as shown and vented via a silicon oil bubbler. Prior to the chamber the gas is bubbled through ethyl alcohol at several controlled temperatures which determine the vapor pressures.

In order to approximate normal spark chamber usage, high energy electrons (about 1.8 MeV max) from a Strontium 90 - Ytrium 90 source traverse two scintillation counters and the spark chamber.

In response to the counters, the coincidence circuit provides an output signal which can be delayed (in addition to the system delay) with calibrated cables. It then triggers a high voltage pulser which applies a negative sparking potential (with less than 5 nsec rise time) to one chamber electrode. This pulse opposes the dc positive clearing or drift field voltage, e.g. 10 to 1000 volts, on the same electrode.

The high voltage pulses and the related occurrence of a spark current are counted in two scalers respectively. An inhibit circuit (not shown) disables the coincidence circuit after each spark, e.g. 10 milliseconds, to insure recovery of the chamber. The average triggering rate was 15 per second.

METHOD AND DISCUSSION

The efficiency of sparking, defined as number of sparks divided by number of particle-triggers, is measured at various time delays between the passage of an ionizing particle through the gap and the application of the high voltage pulse. This, in effect, amounts to testing the gap for the probability of the number of electrons remaining after a selected time while the track electrons are drifting out as shown by t_1, t_2, t_3 in the lower part of Fig. 1.

Assuming a Poisson distribution for the number of electrons in the track, one obtains the well-known relation between a detector efficiency (η) and the number of electrons (n):

$$\eta \approx 1 - \exp(-n)$$

The original number (n_1) of electrons in the track is proportional to the specific ionization (s) ions/cm of the primary particle and the length (ℓ) cm of the track. $n_1 \approx s\ell$. This number is subject to losses, e.g. by drifting out, diffusion, and attachment. The last two losses are assumed small in this particular case, considering drift times below half a microsecond and the nature of the gas.

The losses by drift are proportional to the drift time (T), the drift velocity (v) of unknown distribution, and inversely proportional to the gap length (ℓ). The average number lost is $n_2 \approx \frac{kvT}{\ell} n_1$, where k is a loss factor if losses by attachment or other processes cannot be neglected /10/. Substituting for the remaining number of electrons $n = n_1 - n_2$, the efficiency becomes

$$\eta \approx 1-\exp\left[-s(\ell-kvT)\right]$$

where v and k are functions of the field strength (E) and of gas composition.

If T and ℓ are known experimental parameters, and the fluctuations in s are small, then the efficiency measurement repeated at various (E) and T produces a statistical measure of the disappearance of the last electron. The average drift velocity is then a particular case of this disappearance probability.

The sensitivity is high since the probability from zero to one electron changes the efficiency from 0 to 63%. With this method one can therefore detect small variations in electron disappearance probability.

Subject to the remarks below, one can obtain the velocity and its distribution by varying T. The method can also be applied to measure variations of other gas transport factors as long as these diminish the number of electrons, e.g. electron attachment and diffusion. A drift field may not always be required.

Combinations of disappearance factors can be present. The usual spark chamber operating conditions produce a track with near minimum ionizing particles at nearly normal direction to the electrodes. Under these circumstances there exists an uncertainty in the drift length of the farthest electron and its effective energy. In addition, the original presence of electrons along the whole drift path introduces a bias in velocity measurements because of slow electrons which, however, have shorter path lengths. The relatively short gap can also introduce a bias because equilibrium velocities may not have been achieved for a significant part of the total drift length. Hence, for more precise measurements of gas properties one would use a larger gap and ideally produce a single electron of low energy at a known time and distance, for example, by a different source geometry or by pulsed photoelectric effects on an electrode (e.g. Hurst et al. 1963) /4/. Alternatively, one could produce less than one electron on average and include the production efficiency as a factor in the observed efficiency.

Nevertheless, even with normal nuclear spark chamber operating conditions most of the sensitivity is retained. However, the results that follow should be considered as relative rather than absolute.

RESULTS

The sparking efficiency versus time delay for various electric clearing fields was measured at 12 mmHg ethyl alcohol vapor pressure, as shown in Fig. 2. About 2000 triggering events per point were used. These curves indicate the resolving time and permit selection of operating conditions for nuclear spark chamber applications. Reduction of the clearing time is limited by the onset of gas breakdown at clearing fields above 1200 volts per 6.4 mm. However faster gas mixtures can be made.

From the spacing of the curves one may observe a crowding effect between 200 and 300 nanoseconds. Indeed the delay curves for 200 and 450 volts coincide.

In order to investigate this effect, the efficiency was measured as a function of the field strength at various fixed delays, as shown in Fig. 3.

One outstanding feature is the occurrence of distinct minima and maxima at E/P of about .55 and .92 respectively indicating an opposite variation in drift velocity. The curves below $E/P \approx .4$ do not show this effect indicating a monotonic decrease in drift velocity. At short delays the probability of remaining electrons is large (i.e. above 2) and the method becomes less sensitive. At very low values of efficiency the minima go through zero so that only some of the peaks are seen and the statistics are poor. However, since the delay is an adjustable parameter one can usually bring these effects into focus.

The causes of these effects are discussed later. The variation in drift velocities corresponding to the peaks and valleys are quite small, as may be seen in Fig. 5, which demonstrates the sensitivity of this method.

In order to see the influence of the alcohol, the curves of efficiency versus field strength at various delays were also made at alcohol pressures of 6, 12, 18, 24 and 48 mmHg with only 1000 events per point. These sets of curves (not shown) resemble in shape those of Fig. 3. Minima and maxima are seen in all of them although their locations differ.

The shift in field strength at which the minimum (or maximum) occurs with increasing alcohol pressure is plotted in Fig. 4. The increase in field strength is nearly linear and is a consequence of the reduction of the mean free path with an increasing number of alcohol molecules, thus requiring a corresponding increase in field strength to achieve the minimum (or maximum).

DRIFT VELOCITIES AND DISCUSSION

The drift velocities can be derived from curves as in Figs. 2 and 3 by an appropriate selection of the efficiency value for which the average velocities are to be obtained. Since the electron velocity distribution in this case is not well known, the 50% efficiency (.7 electrons present) was chosen so that approximately half the electrons have a higher velocity. This average drift velocity at any E/P is then approximately equal to the delay where the 50% line crosses all the curves divided by the gap length (neglecting losses by attachment). The resultant drift velocity curves versus E/P from .1 to 2 are shown in Fig. 5 for alcohol pressures of 6, 12, 18, 24 and 48 (mmHg). For comparison also, the pure neon velocities from the literature /5/ are indicated. A one-point check in neon + 10% helium without alcohol was in reasonable agreement with this neon curve considering the somewhat lower drift velocity in helium.

Several factors are apparent from the curves and will be discussed (qualitatively only) by reference to cross-section data from the literature /6/, collected in Fig. 6, on the components in the gas mixture. The neon and the helium cross-sections have been multiplied by 10 to make them visible in the presence of the large alcohol cross-sections.

a) All drift velocities in the mixture are several times faster than in pure neon.

From the classical mobility theory (which in the case of electrons is only sufficient for a qualitative indication) the drift velocity v_d is proportional to the field strength, the mean free path (λ), and inversely proportional to the average agitation velocity (u).

$$v_d \approx \frac{e}{m} \frac{E}{P} \frac{\lambda}{u}$$

Because of the low lying excitation levels in molecular gases relative to those of noble gas atoms, the agitation energy is greatly decreased by inelastic collisions. In addition, the collision cross-section for neon decreases at lower electron energies which means an increase in mean free path. (The helium cross-section actually rises and therefore partly cancels the decrease in cross-section.) Both previous factors tend to increase the drift velocity over that of the pure neon. This type of behavior has often been observed for molecular gas admixtures /7/ to argon and heavier noble gases, which have a strong Ramsauer cross-section minimum.

b) The velocities in the rising parts of the curves below the peaks are faster when the alcohol pressure is lower because the effective mean free path (λ) increases with fewer alcohol molecules.

c) At the peaks the velocities are higher when the alcohol pressures are higher. These peaks require increasing values of the electric field (see Fig. 4) in order to bring the effective electron velocity to the same levels. However, since the effective mean free path decreases, the average velocity is higher.

d) The peak mobility $v/_{E/P}$ (calculated from Fig. 5), which indicates the ratio of the mean free path to the agitation velocity, also decreases with increasing alcohol concentration.

Alcohol Pressure	6	12	18	24	(mmHg)
Approx. Mobility at Peak	6.7	5.9	4.7	3.5	cm^2/Volt-μsec

e) The velocity peaks, which are more clearly visible as minima in the sensitive efficiency curves, are probably due to a minimum in the collision cross-section for alcohol /6/ (Fig. 6). However an effect due to attachments to alcohol or its dissociation products is not completely ruled out. Since the agitation velocity and its distribution in the mixture was not known, a direct correlation was not possible. However recent cross-section /6/ and drift velocity data /8/ in neon for low energies show only a continuous smooth reduction with energy. The cross-section curve for helium on the other hand smoothly rises with reduction of electron energy and then

diminishes at very low energies. A composite cross-section curve weighted according to component pressures would still leave the alcohol minimum as the predominant effect.

English and Hanna (1953) /7/ attribute velocity peaks in noble gas mixtures with CO_2 to the Ramsauer minima in the heavier noble gases and to a lesser extent in neon, and not to the effect of the moderating gas. Observation by others of electron clearing times in nuclear spark chambers have shown a minimum of efficiency for neon (Cronin & Renninger 1960) /9/ which may have been caused by impurities released in the chamber, as some other users did not find this effect in neon. Observation in somewhat impure neon with about 60 mmHg alcohol (Burnham et al. 1963) /10/ also did not show the effect which, as the present work indicates, would fall outside their range. Mixtures of neon + 35% helium were used by Hohne and Schneider (1963) /11/. They did not find such effects in the pure gas but an efficiency minimum appeared with addition of O_2, presumably due to a combination of collision and attachment cross-section variation.

The method of investigating electron transport phenomena by variation in the disappearance probability of an electron is very sensitive, and therefore requires care to keep the desired phenomena in the measuring range. Disappearance can be due to a combination of factors.

REFERENCES

/1/ W. A. Wenzel, Annual Review of Nuclear Science 14, 205 (1964) (Annual Rev. Inc., Palo Alto, Calif.)

G. Charpak, L. Massonnet, Progress in Nuclear Techniques 1, 323 (1965) (North-Holland Publishing Co.)

/2/ The neon-helium mixture is used in spark chambers because it is cheaper than pure neon. Alcohol can be added for quenching and reduction of recovery time after a spark. See for example: J. Fischer, Digitized Discharge Planes and Their Operation at Rapid Rates, Purdue Conference on Instrumentation for High Energy Physics, To be Published in: IEEE Transactions on Nuclear Science, NS 12, No. 5 August 1965

/3/ Aluminum is not the best choice. The surface deteriorated with use, causing breakdown at the higher drift fields.

/4/ A complementary method by Hurst et al. measures drift times of single electrons detected by a Geiger counter at the end of the drift space.

G. S. Hurst et al., J. Chem. Phys. 39, 1341 (1963)

/5/ a) J. C. Bowe, Phys. Rev. 117, 1411 (1960)

b) Townsend and Bailey in R. H. Healey and J. W. Reed, The Behavior of Slow Electrons in Gases, p. 89 (1941)

/6/ Alcohol: F. Schneider, Z. Electrochem. 36, 700 (1930) (in S. C. Brown, Basic Data of Plasma Physics, p. 13 Wiley (1959))

Neon and Helium: H. Massey and E. Burhop, Electronic and Ionic Impact Phenomena, p. 10 Oxford (1952)

A. V. Phelps et al., Phys. Rev. 84, 559 (1951)

/7/ W. N. English and G. C. Hanna, Can. J. Phys. 31, 768 (1953)

T. E. Bortner, G. S. Hurst, W. G. Stone, Rev. Sci. Instr. 28, 103 (1957)

F. Schneider and K. Hohne, Nucl. Instr. Meth. 20, 152 (1963)

/8/ J. L. Pack, A. V. Phelps, Phys. Rev. 121, 798 (1961); 127, 2084 (1962)

/9/ J. W. Cronin and G. Renninger, Rev. Sci. Instr. 32, 496 (1961)

/10/ J. U. Burnham et al., J. Sci. Instr. 40, 296 (1963)

/11/ K. Hohne and F. Schneider, CERN AR/Int.GS/63-6 (1963) (Unpublished)

Figure Captions

Fig. 1 Pulsed nuclear spark chamber system. Spark pulse opposes drift of track electrons.

Fig. 2 Resolving time curves. Spark chamber efficiency as a function of drift time at various clearing fields.

Fig. 3 Spark chamber efficiency as a function of E/P at various drift times showing minima and maxima.

Fig. 4 Changes in required E/P at efficiency minima and maxima as a function of alcohol pressure.

Fig. 5 Approximate electron drift velocities in the gas mixture as a function of E/P for various alcohol pressures compared with neon only.

Fig. 6 Collision cross-sections from the literature in ethyl alcohol, neon, and helium as a function of the electron agitation velocity; and the electron agitation velocity as a function of E/P in neon.

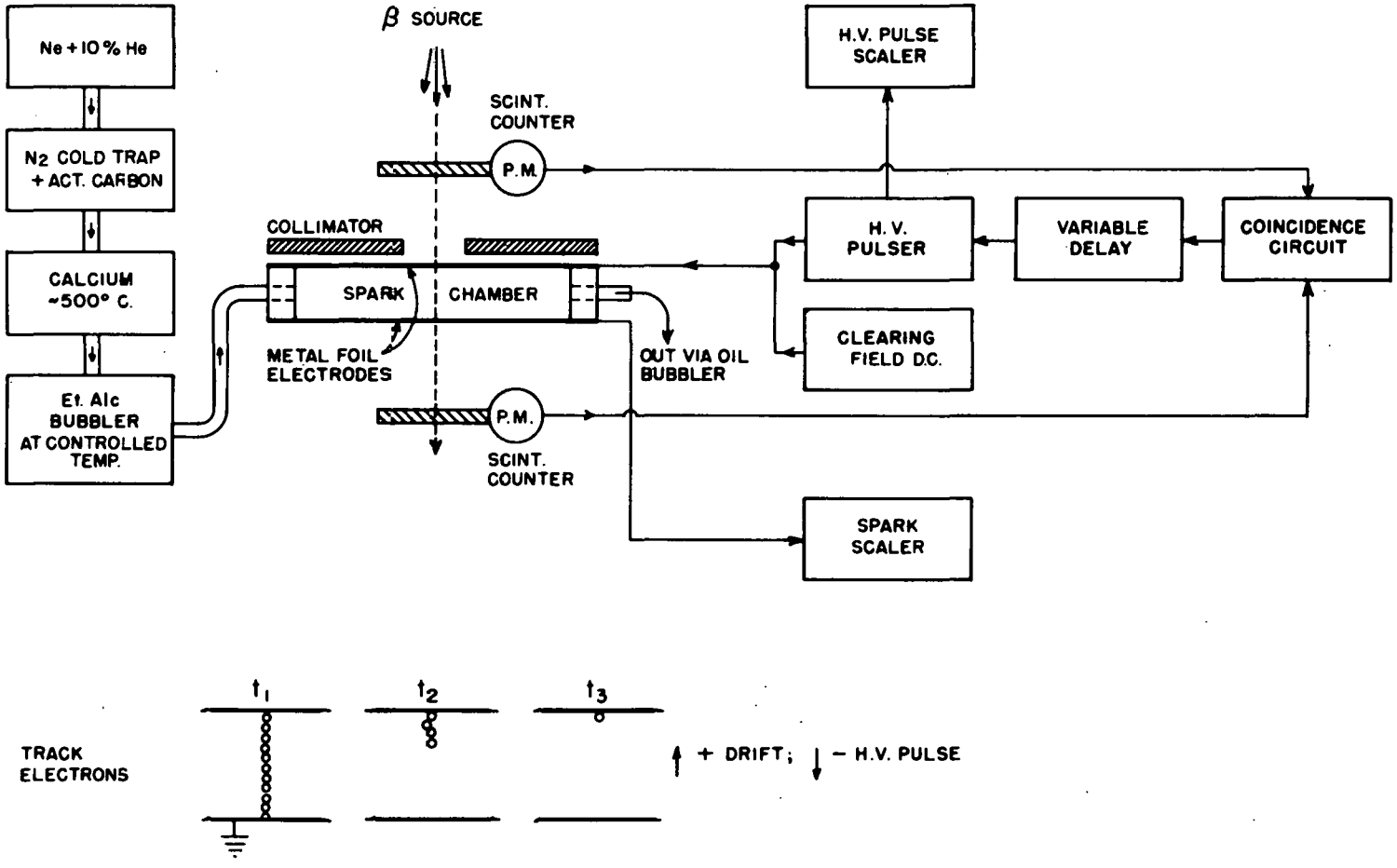

PULSED NUCLEAR SPARK CHAMBER SYSTEM

FIGURE 1

Pulsed nuclear spark chamber system. Spark pulse opposes drift of track electrons.

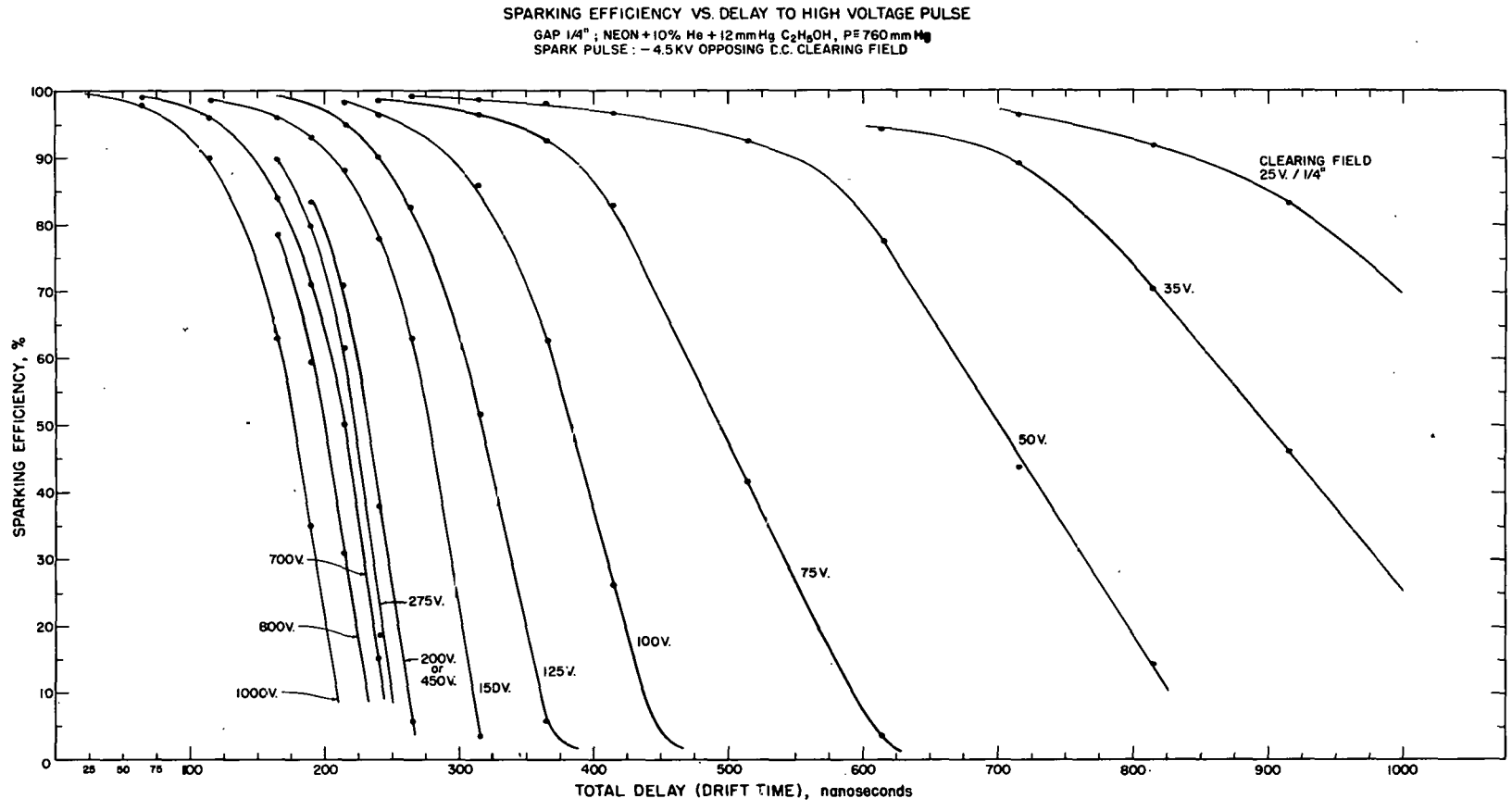

FIGURE 2

Resolving time curves. Spark chamber efficiency as a function of drift time at various clearing fields.

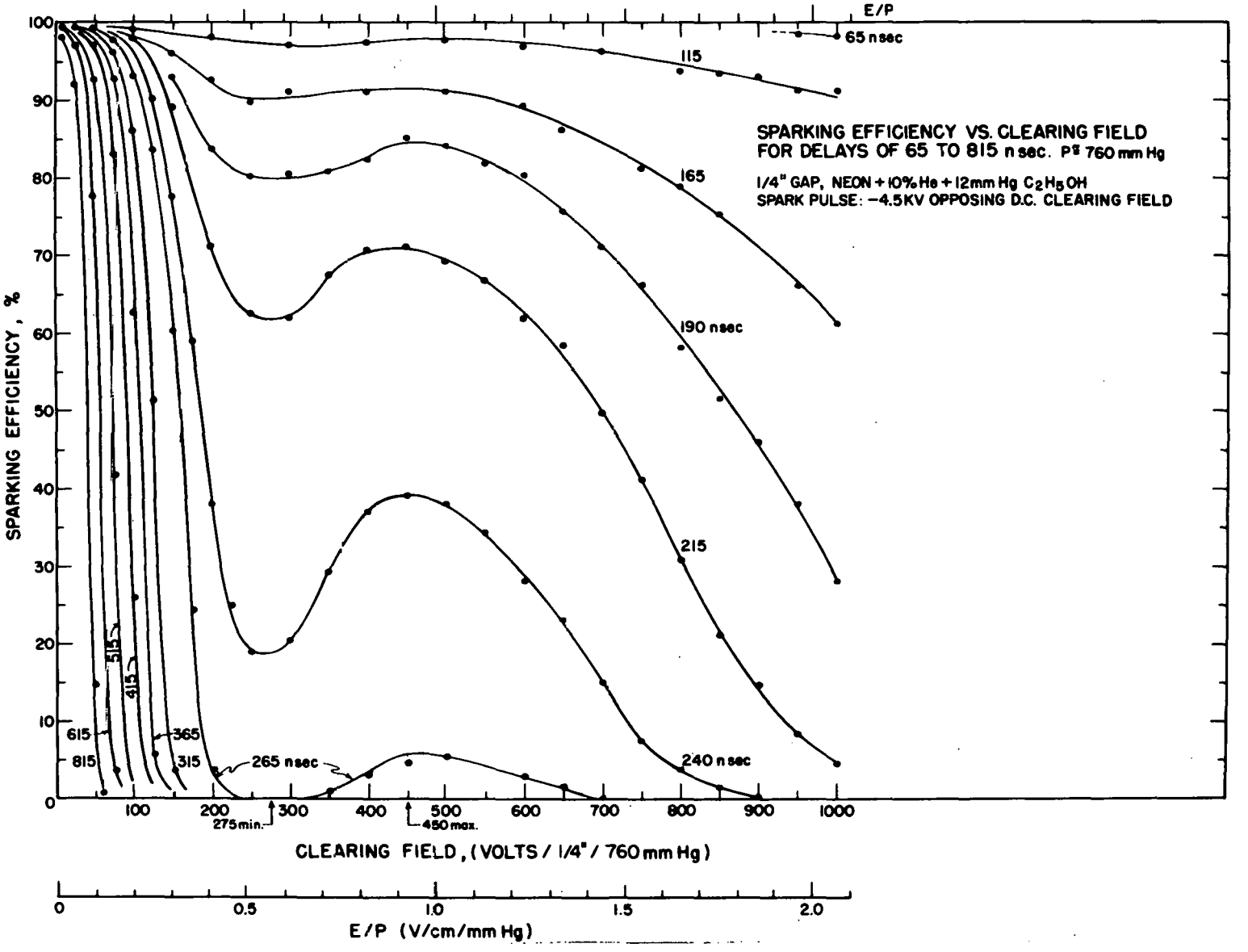

FIGURE 3

Spark chamber efficiency as a function of E/P at various drift times showing minima and maxima.

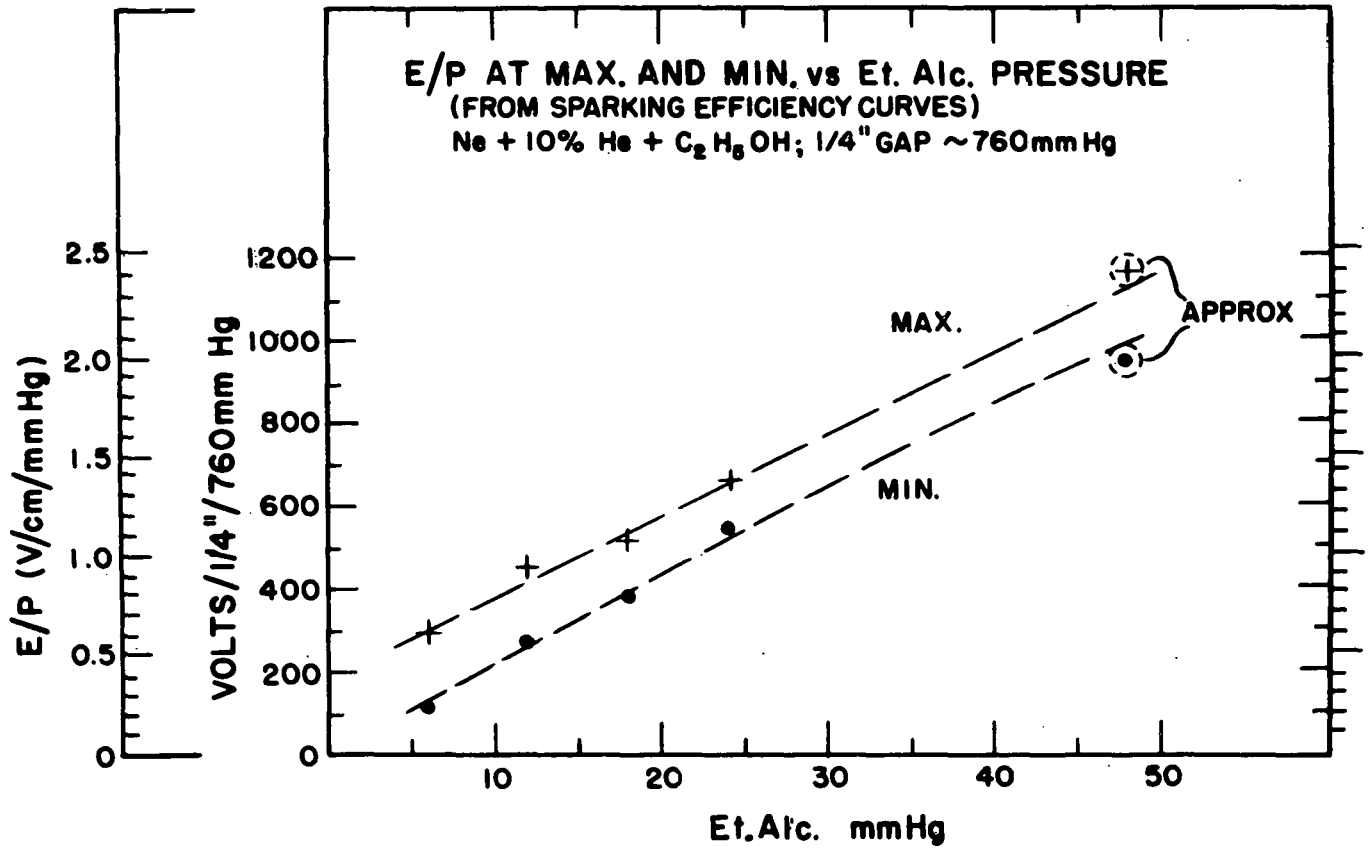

FIGURE 4

Changes in required E/P at efficiency minima and maxima as a function of alcohol pressure.

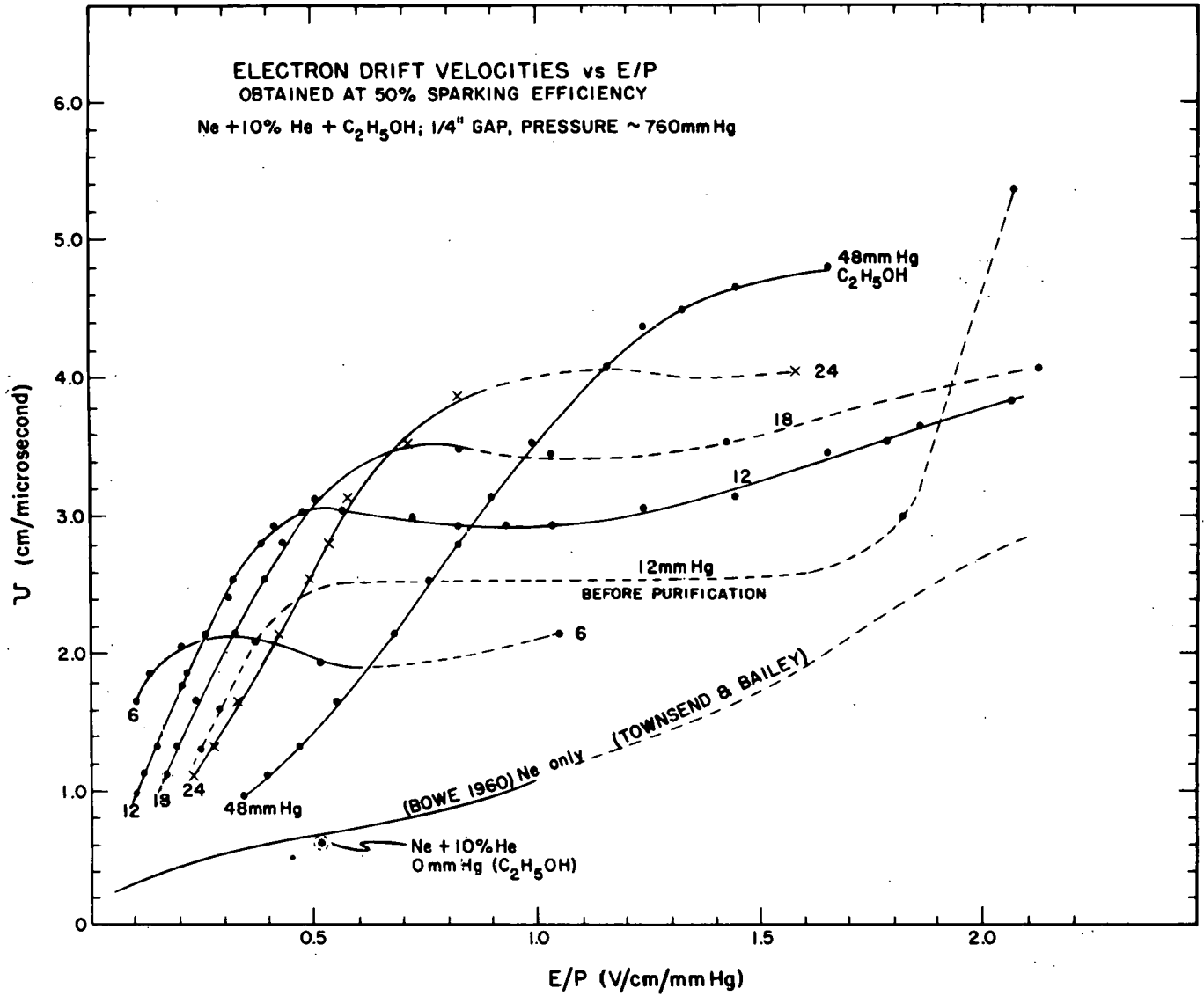

FIGURE 5

Approximate electron drift velocities in the gas mixture as a function of E/P for various alcohol pressures compared with neon only.

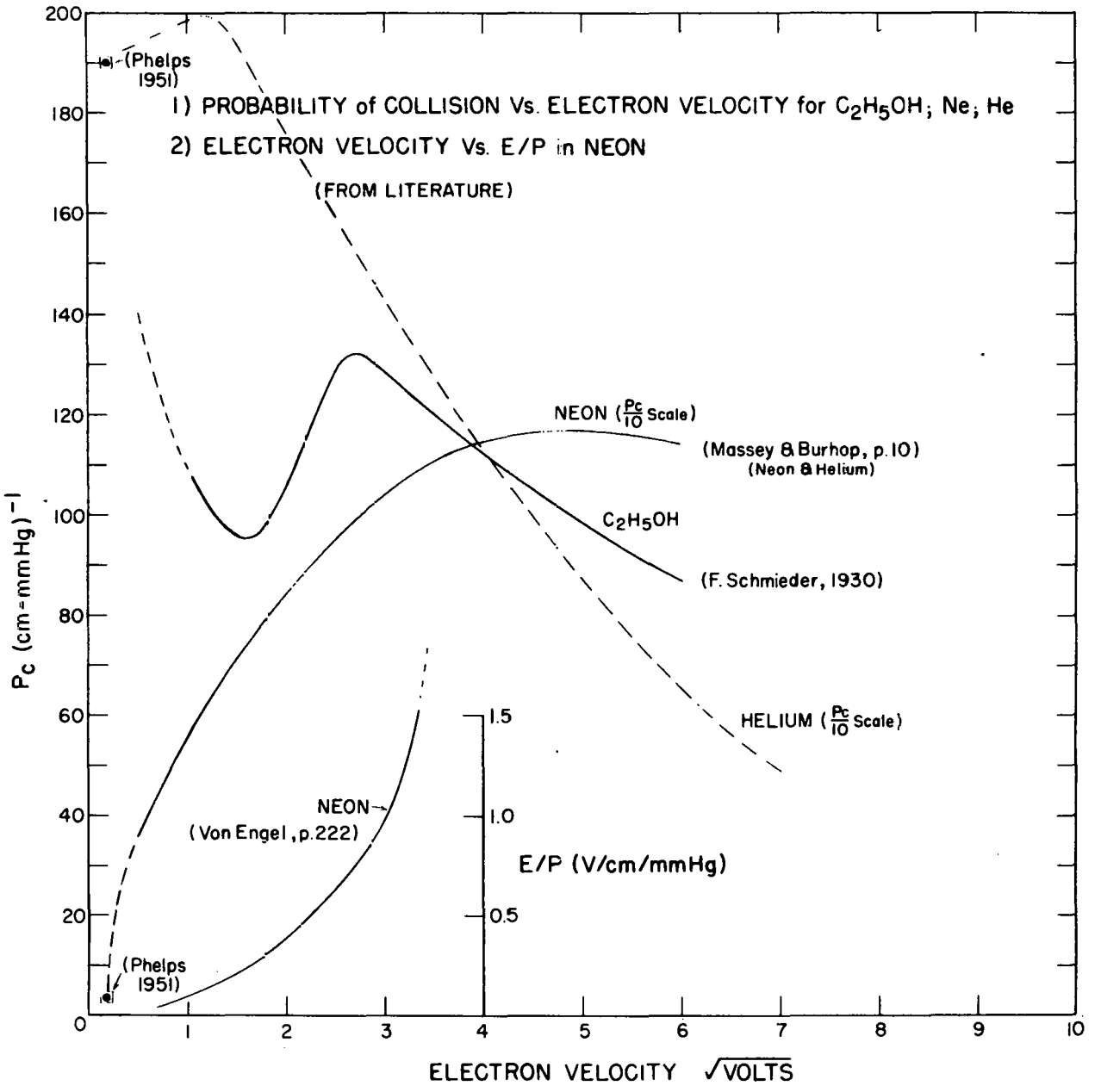

FIGURE 6

Collision cross-sections from the literature in ethyl alcohol, neon, and helium as a function of the electron agitation velocity; and the electron agitation velocity as a function of E/P in neon.